PERGAMON

Radiation Physics and Chemistry 60 (2001) 405–410

Radiation Physics and Chemistry

www.elsevier.com/locate/radphyschem

Formation, trapping and kinetics of H atoms in wet zeolites and mesoporous silica☆

S.C. Chemerisov, D.W. Werst, A.D. Trifunac*

Chemistry Division, Argonne National Laboratory, 9700 Cass Avenue, Argonne, IL 60439, USA

Abstract

Pulse radiolysis and time-resolved EPR were used to study mobile H atoms in wet porous solids, including zeolites and mesoporous molecular sieves. The time-resolved study was accompanied by measurements of trapped H atoms at low temperatures. Radiolytic H atoms arise from both the solid matrix and adsorbed water. Under conditions of high dose rate, the H atoms mainly decay by reaction with matrix defects. An interesting detail of H atom diffusion in these systems is the apparent segregation into different "phases". The different phases can be silica and water (MCM-41) or they can be different pore systems in the solid (Y zeolite). Published by Elsevier Science Ltd.

Keywords: H atoms; Zeolite; MCM-41; Radiolysis; EPR

1. Introduction

The formation and reactions of H atoms under radiolysis of glasses (Griscom, 1985; Tsai and Griscom, 1988; Tsai et al., 1989; Saeki et al., 1985; Miyazaki et al., 1984), semiconductor/oxide interfaces (Radzig, 1998; Edwards et al., 1994; Stahlbush et al., 1993; Bobyshev et al., 1990), and wet porous solids (Nakashima and Masaki, 1996; Nakashima and Aratono, 1993) have been subjects of interest because of their importance in understanding the fundamental processes of energy transfer, charge trapping, defect repair and gas evolution in such systems. H atoms are useful probes of the chemistry affecting the long-term stability of vitrified high-level waste (HLW) forms, and the fate of H atoms in HLW impacts both the evolution of matrix defects and the radiation chemical yield of hydrogen gas that can lead to the formation of gas bubbles and other undesired effects in HLW glasses (Griscom, 1985; Tsai and Griscom, 1988; Tsai et al., 1989; Saeki et al., 1985). During long-term storage of HLW, it is expected that exposure to water will introduce an additional source of radiolytic H atoms that should be taken into account in any prediction of the long-term stability of the waste form.

Two mechanisms are responsible for the formation of H atoms in the radiolysis of water (Schwarz 1969). Ionization of water is rapidly followed by proton transfer from H_2O^+ to surrounding water molecules to give hydroxyl radical and a hydronium ion, H^+_{aq}. The recombination reaction involving H^+_{aq} and hydrated electron leads to H atoms. H atoms also result from the fragmentation of excited water molecules formed via direct excitation or via recombination of electron–hole pairs. Bimolecular recombination of H atoms accounts for most of the H atom decay in liquid water or ice (Bartels et al., 1989; Han and Bartels, 1991).

The source of radiolytic H atoms in the prototypical glass, fused silica, are hydroxyl impurities (≡Si–OH) (Bartels et al., 1987). Synthetic silicas that contain a relatively high concentration of these silanol groups are sometimes called "wet" silica. The predominant H atom formation mechanism in wet silica is the decay of triplet excitions in reactions with silanol groups, Eq (1). A variety of defects occur simultaneously with the H atoms in silica and, especially at high radiation dose rates, the

☆Work at Argonne performed under the auspices of the Office of Basic Energy Sciences, Division of Chemical Science, US-DOE under contract number W-31-109-ENG-38.

*Corresponding author. Fax: +1-630-252-4993.

E-mail address: trifunac@anl.gov (A.D. Trifunac).

0969-806X/01/$ - see front matter Published by Elsevier Science Ltd.
PII: S0969-806X(00)00408-4

reactions with defects are largely responsible for the decay kinetics of H atoms Eqs. (2)–(4) (Shkrob and Trifunac, 1996; Shkrob and Trifunac, 1997). Likewise, the thermal annealing and steady-state concentrations of defects in silica and other glasses are strongly dependent on the action of radiolytic H atoms.

$$^3\text{exciton} + \equiv \text{SiOH} \rightarrow \equiv \text{SiO}^\bullet + \text{H}, \quad (1)$$

$$\equiv \text{SiO}^\bullet + \text{H} \rightarrow \equiv \text{SiOH}, \quad (2)$$

$$\equiv \text{Si}-\text{Si} \equiv +2\text{H} \rightarrow \equiv \text{SiH HSi} \equiv \quad (3)$$

$$\equiv \text{Si}^\bullet + \text{H} \rightarrow \equiv \text{SiH} \quad (4)$$

In the present work, we have undertaken to study H atoms in radiolysis of systems in which silicate solids and water are in intimate contact. We take as our models microporous zeolites (NaX, NaY and HY) and mesoporous silica (MCM-41). The potential sources of H atoms are both the structural silanol groups of the solid and water adsorbed inside the pores. In the case of HY zeolite, reactions of electrons with acidic protons that occur at bridging hydroxyl sites (≡S–O(H)-Al≡), Eq (5), are an additional source of H atoms.

$$(\equiv \text{S}-\text{O(H)}-\text{Al} \equiv) + \text{e}^- \rightarrow \equiv \text{Si}-\text{O}^{(-)} - \text{Al} \equiv +\text{H}. \quad (5)$$

Pulse radiolysis with time-resolved EPR was applied to study the formation and decay kinetics of H atoms in the wet solids and this information was complemented by measurements of trapped H atoms at low temperature by continuous wave EPR. The main questions that we address are the following: (1) How are H atoms produced and where do they come from? (2) What is the dominant fate of H atoms? (3) What is the role of the solid–water interface in the radiation chemistry? (4) Is the water inside the porous solids like bulk water with regard to H atom behavior, e.g. trapping?

2. Experimental section

Zeolite NaX was obtained from Aldrich; zeolites NaY and HY were received from UOP. Silica MCM-41 was synthesized by a microwave-heating method (Wu and Bein, 1996). The resulting solid gave an XRD powder pattern with four well-defined peaks which can be indexed with 1 0 0, 1 1 0, 2 0 0 and 2 1 0 in hexagonal symmetry. After the surfactant was removed by calcination at 540°C the d_{100} value was 33 Å, which translates to a pore diameter of slightly less than 3 nm.

The solid powders in Pyrex or Suprasil tubes were evacuated and heated under vacuum (10^{-4} Torr) prior to adsorbing water. The temperature program was: 30 min at room temperature, ramp to 450°C over a 2 h period, hold at 450°C for 4 h, cool to room temperature. Water was degassed by four freeze–pump–thaw cycles. Dehydrated powders were saturated with water by overnight equilibration with approximately 20 Torr of water vapor. By this procedure the MCM-41 was estimated to adsorb 35% water by weight and the zeolites approximately 25%. After water adsorption the samples were pumped at dry ice temperature and then sealed. Xenon was added prior to sealing to improve the thermal conductivity of the samples used for pulse radiolysis. The Xe remained liquified during all experiments. The temperature rise induced by electron beam irradiation in time-resolved experiments was less than 2 K.

Deuterium exchange of the HY zeolite was accomplished by equilibrating the dehydrated zeolite with 500 Torr D_2 at 450°C for 4 h. During the exchange procedure the D_2 atmosphere was evacuated and replaced three times. From the relative EPR intensities of trapped H and D atoms in the deuterium-exchanged zeolite we estimate approximately 40% exchange.

First-derivative, continuous-wave EPR spectra were measured (Bruker ESP 300E spectrometer, operating at 9.44 GHz) after sample irradiation with 3 MeV electrons from a Van de Graaff accelerator at 77 K. The empty half of the sample tube was flame-annealed while the powder remained immersed in liquid nitrogen so that signals from trapped H atoms and radiation-induced defects in the tube were removed. The tube was then inverted under liquid nitrogen. For measurements of trapped H(D) atoms below 77 K in situ experiments were done, where the sample was irradiated directly in the liquid helium dewar used for temperature control in the EPR spectrometer. For in situ experiments D_2O and D-exchanged zeolite were used to discriminate contributions from H atom signals in the sample tubes and Suprasil dewar. Special care was taken to avoid microwave power saturation and over modulation of the EPR spectra.

Time-resolved EPR spectra were obtained using a homebuilt pulsed EPR spectrometer (Trifunac et al., 1979). The microwave pulse was synchronized to the electron beam pulse from the Van de Graaff accelerator. The dose per pulse was varied by varying the length of the electron beam pulse (12–100 ns). Typically, a 100 ns electron beam pulse of 40 nC resulted in a dose of 20 Gy/pulse to the sample. For time-resolved experiments Pyrex sample tubes were used to avoid spurious contributions to the H atom signal in the irradiated powder. The sample temperature was regulated by flowing cold nitrogen gas through a cooling jacket also constructed of Pyrex.

Upon excitation with a single microwave pulse the magnetization of H atoms oscillates in the time domain (free induction decay or FID) as in Fig. 1. Field-swept spectra were obtained by integration of part of the FID using boxcar averaging. The resulting EPR spectra consist of modulated lineshapes of the type shown in the

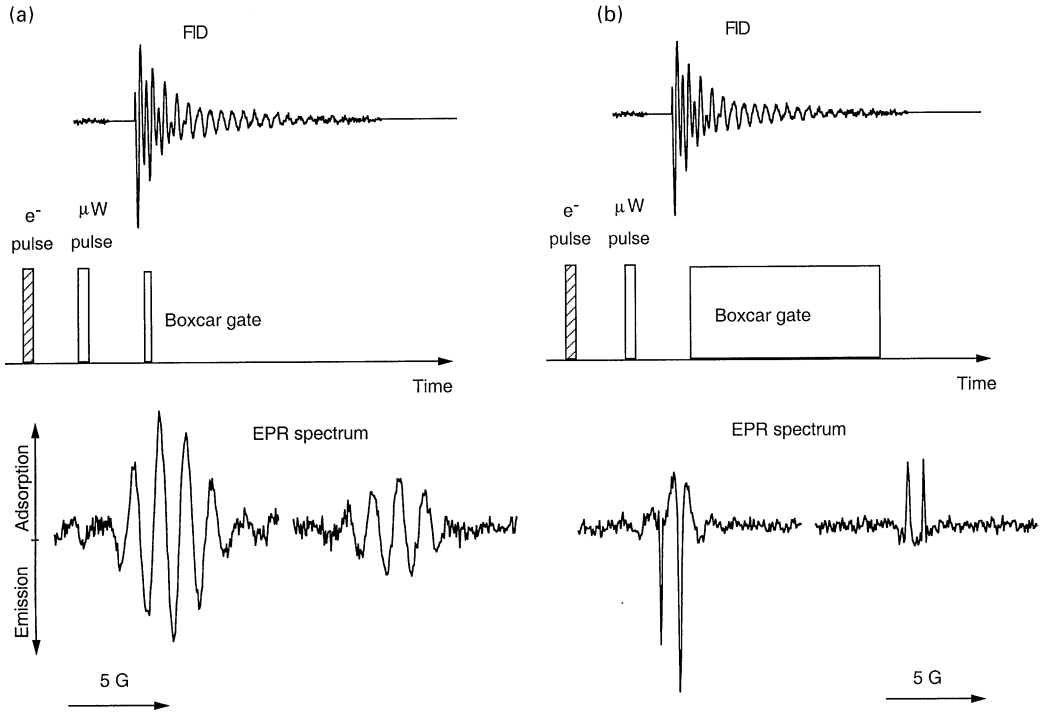

Fig. 1. Pulsed EPR experiment with FID detection. The low field ($m_I = 1/2$) and high field ($m_I = -1/2$) resonances of the H atom are shown side by side. The actual separation is ca. 505 G.

lower half of Fig. 1a. To resolve two different H atom signals with slightly different hyperfine coupling constants the FID was integrated with a wide enough boxcar gate (~1.5 μs) to give a narrow resonance line (Fig. 1b).

3. Results and discussion

3.1. Transient H atoms

Mobile H atoms were observed by time-resolved EPR within 10^{-8}–10^{-4} s after generation by the electron beam pulse. These H atoms exhibit nonthermal population of electron spin states because of chemically induced dynamic electron polarization (CIDEP) (Freed and Pedersen, 1976; Adrian, 1979). Time-resolved EPR spectra of H atoms in water-saturated NaY and NaX are presented in Fig. 2. There was little change in the spectra over the temperature range studied (200–260 K). All spectra show the E/A pattern: low-field component in emission and high-field component with enhanced absorption. This type of polarization is indicative of the ST_0 and ST_- radical pair mechanisms (RPM) of CIDEP (Shkrob and Trifunac, 1996). For H atoms the ST_0

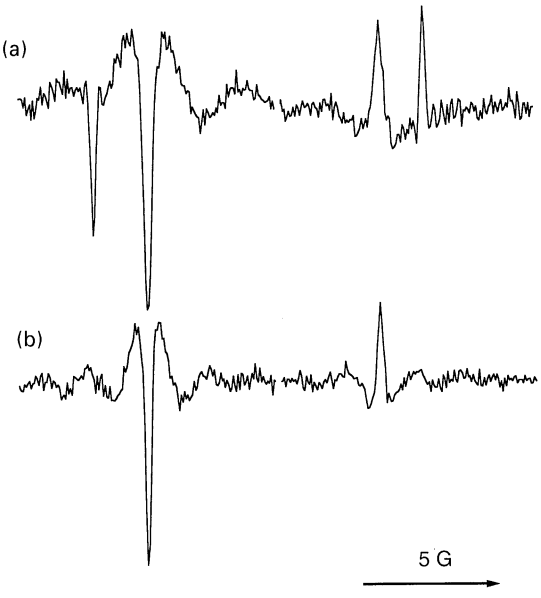

Fig. 2. Time-resolved EPR spectra of transient H atoms measured at 248 K. (a) Water-saturated NaY, (b) water-saturated NaX. The time delay between the 100 ns electron beam pulse and the microwave pulse was 1 μs.

mechanism gives E/A polarization with equal intensities. The ST_ mechanism is observed because of the large hyperfine coupling constant of H atoms. It gives emission for the low field component. Together these two polarization mechanisms give E/A polarization with greater intensity in the low field component compared to the high field component.

In NaY zeolite two transient H atom signals with different hyperfine coupling constants were detected. This observation is evidence of H atoms moving in different domains that do not exchange on the timescale of the experiment. The designation of the different domains is suggested by the structure of the zeolite, which consists of supercages and smaller sodalite cages. Water can interpenetrate both types of cage. Thus there is no distinct aqueous and nonaqueous phase. Alternatively, one can define two separate spaces as (1) the sodalite cages, interconnected by double six-member rings, and (2) the supercages, which communicate with each other via windows of 7.4 Å diameter. It is quite conceivable that the potential governing H atom diffusion confines H atoms to one or the other of these domains for significant lengths of time.

Only one transient H atom signal was observed in NaX zeolite. The lower Si/Al ratio of NaX (1.0 compared to 2.5 for NaY) translates to a higher Na^+ concentration in NaX by the same factor. It is known that upon hydration Na^+ migrates from sodalite cages to supercages (Motier, 1985). Thus in water-saturated NaY the Na^+ concentration is higher in the supercages than in the sodalite cages. The Na^+ cation concentration will be more equalized between the supercages and sodalite cages in NaX because the Na^+ loading is greater. If the high concentration of Na^+ is the primary cause of modulation of the H atom hyperfine coupling constant, then these facts provide a way to rationalize the observation of two hyperfine components and one hyperfine component in NaY and NaX, respectively, — assuming as above that the H atoms diffuse preferentially in chains of sodalite cages or from supercage to supercage.

We observed two transient H atom signals in water-saturated MCM-41 as well. The signal-to-noise of the EPR spectrum in MCM-41, however, was inferior to that obtained in the zeolite samples and there was evidence that the MCM-41 structure was less immune to degradation caused by the large cumulative doses ($>10^7$ Gy) necessary to collect the transient H atom spectrum. In all cases the EPR spectrum showed some evolution during the first hours of irradiation. For the zeolites, the EPR spectrum eventually ceased to evolve and the spectra in Fig. 2 are representative of these data collected after long irradiation. For MCM-41 the signal intensity also decayed with cumulative dose, which was the limiting factor. The XRD powder pattern of irradiated MCM-41 showed evidence of contraction of the pore size (10–15%) and loss of hexagonal ordering.

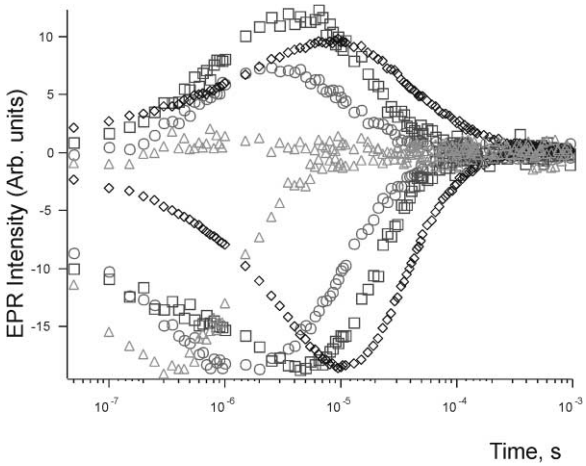

Fig. 3. Kinetics of H atom magnetization in wet solids: MCM-41 (triangles), NaY (squares for H atoms with higher splitting and circles for lines with smaller splitting) and bulk ice (rhombs). The signal from the high field line is in absorption and the low field line is in emission.

Nevertheless, we have a clue that H atoms diffuse in two separate domains in MCM-41. Unlike the zeolites, the intuitive separation in MCM-41 is between aqueous and silica phases, that is, the water-filled pores and the silica walls, which are typically found to have a thickness of ca. 1 nm.

The H atom CIDEP kinetics observed at 250 K in MCM-41, NaY and NaX are shown in Fig. 3. Results for ice are shown for comparison. The kinetics were not temperature dependent over the temperature range 200–260 K in contrast with bulk ice and pure silica. The H atom signals decayed faster in MCM-41 and in zeolites than in bulk ice and the decay times were independent of the adsorbed dose per pulse (electron beam pulse width). Both of these observations imply that the H atoms do not decay simply by combination with other H atoms. The principal reaction partners with H atoms are the radiation-induced defects at the water–silicate interface.

Attempts to observe transient H atoms in dry powders failed in every case, even when trapping studies (vide infra) indicated the formation of H atoms in the absence of water.

3.2. Trapped H atoms

We studied trapping of H atoms during radiolysis at 77 and 15 K to further elucidate the source of H atoms. The dose needed to observe trapped H atoms was naturally smaller than the cumulative dose in the pulsed

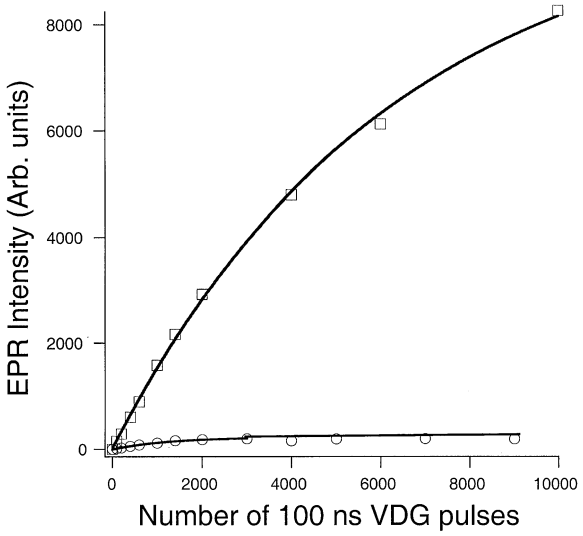

Fig. 4. Dose dependence of the trapped D atom yield in DY zeolite (squares) and DY zeolite saturated with SF_6 (circles).

EPR experiments. The continuous wave EPR spectra were collected after doses of approximately 10^6 Gy or less.

As have others, we observed strong signals from trapped H(D) atoms in dehydrated H(D)Y zeolite at 77 and 15 K. The zeolite lattice provides sufficient trapping sites for H atoms. No trapped H atoms were observed in NaY zeolite, which indicates that the main source of H atoms from the dry zeolite are the acidic framework hydroxyl groups (≡S–O(H)–Al≡). This source of H(D) atoms, Eq (5), is strongly quenched by the addition of an electron scavenger like SF_6 (Fig. 4). The EPR intensity from trapped H atoms in dry MCM-41 was almost undetectable, approximately three order of magnitude weaker than in amorphous silica gel.

The observation of strong signals from trapped D atoms at 77 and 15 K in NaY with adsorbed D_2O, together with the result for the dry zeolite, confirms that the source of H(D) atoms in this system is the adsorbed water. MCM-41 with adsorbed D_2O gave only very weak signals from trapped D atoms at 77 K, but strong signals at 15 K — comparable to that in bulk D_2O at 15 K. It is well known that H atoms are not trapped in ice at 77 K.

Finally, we showed that MCM-41, as expected, is a source of radiolytic H atoms by the following experiment. Deuterium-exchanged MCM-41 saturated with Ar or Xe was irradiated at 15 K and under these conditions strong intensity from trapped D atoms was observed. We can conclude that the vanishingly small signals from trapped H(D) atoms in dry MCM-41 is due to poor trapping and not to low yields of H(D) atoms.

4. Conclusions

This ongoing study allows several important conclusions:

- Radiolytic H atoms derive from both the solid matrix and adsorbed water.
- Zeolites are better traps for H atoms than MCM-41 or the small pools of water inside the MCM-41 pores.
- The kinetics of H atoms in porous media is very different from that of bulk ice. The main reactions of H atoms in porous media are presumably with metastable defects in the solid and not H–H combination. This finding has significant implications for the generation of H_2 in HLW waste forms, and the role of H atoms in annealing radiation induced defects in glass forms.
- Mobile H atoms can remain "phase segregated". Examples include aqueous and silica phases in contact, like in MCM-41, and different pore systems in the same zeolite.

Acknowledgements

We acknowledge J. Gregar for constructing the glass vacuum manifold and supplying the EPR tubes and R. H. Lowers for his continuing support in operating the Van de Graaff accelerator.

References

Adrian, F.J., 1979. Principles of the radical pair mechanism of chemically induced nuclear and electron spin polarization. Rev. Chem. Intermed. 3 (1–2), 3–43.

Bartels, D.M., Werst, D.W., Trifunac, A.D., 1987. Hydrogen atom diffusion and CIDEP in room temperature fused silica. Chem. Phys. Lett. 142 (3–4), 191–195.

Bartels, D.M., Craw, M.T., Han, P., Trifunac, A.D., 1989. Hydrogen/deuterium isotope effects in water radiolysis. 1. The mechanism of chemically induced dynamic electron polarization generation in spurs. J. Phys. Chem. 93 (6), 2412–2421.

Bobyshev, A.A., Radtsig, V.A., Senchenya, I.N., 1990. Free radical centers of the predetermined structure on silica surface and their reactivity in substitution reactions. II.–Si–,–SiOO–graft hydrocarbon radicals. Kinet. Katal. 31 (4), 931–938.

Edwards, A.H., Pickard, J.A., Stahlbush, R.E., 1994. Interaction of hydrogen with defects in amorphous silica (a-SiO2). J. Non-Cryst. Solids 179, 148–161.

Freed, J.H., Pedersen, J.B., 1976. The theory of chemically induced dynamic spin polarization. Adv. Magn. Reson. 8, 1–84.

Griscom, D.L., 1985. Diffusion of radiolytic molecular hydrogen as a mechanism for the post-irradiation buildup of

interface states in silica-on-silicon structures. J. Appl. Phys. 58 (7), 2524–2533.

Han, P., Bartels, D.M., 1991. Hydrogen/deuterium isotope effects in water radiolysis. 3. Atomic hydrogen in acidic water/water-D2 mixtures. J. Phys. Chem. 95 (23), 9370–9374.

Miyazaki, T., Azuma, N., Fueki, K., 1984. Kinetic behavior of hydrogen and deuterium atoms in– -irradiated silica as studied by ESR spectroscopy. J. Am. Ceram. Soc. 67 (2), 99–102.

Motier, W.J., 1985. Compilation of Extra Framework Sites in Zeolites. Butterwoth Scientific Ltd., London, 19.

Nakashima, M., Aratono, Y., 1993. Radiolitic hydrogen gas formation from water adsorbed on type A zeolite. Radiat. Phys. Chem. 41 (3), 461–465.

Nakashima, M., Masaki, N.M., 1996. Radiolitic hydrogen gas formation from water adsorbed on type Y zeolite. Radiat. Phys. Chem. 47 (2), 241–245.

Radzig, V.A., 1998. Point defects in disordered solids: Differences in structure and reactivity of the (≡Si–O)2Si: groups on silica surface. J. Non-Cryst. Solids 239 (1–3), 49–56.

Saeki, M., Ohno, S., Tachikawa, E., Azuma, N., Miyazaki, T., Fueki, K., 1985. Comparison of 80 keV deuterium (+) ion implantation with thermal molecular deuterium doping in silica by FTIR and ESR spectroscopy. J. Am. Ceram. Soc. 68 (3), 151–155.

Schwarz, H.A., 1969. Application of the spur diffusion model to the radiation chemistry of aqueous solutions. J. Phys. Chem. 73 (6), 1928.

Shkrob, I.A., Trifunac, A.D., 19961. Time-resolve EPR of spin-polarized mobile H atoms in amorphous silica, the involment of small polarons. Phys. Rev. B 54, 5073.

Shkrob, I.A., Trifunac, A.D., 1997. Time-resolve EPR of spin-polarized mobile H atoms in amorphous silica, the involment of small polarons. Phys. Rev. B 54, 15073.

Stahlbush, R.E., Edwards, A.H., Griscom, D.L., Mrstik, B.J., 1993. Post-irradiation cracking of hydrogen and formation of interface states in irradiated metal-oxide-semiconductor field-effect transistors. J. Appl. Phys. 73 (2), 658–667.

Trifunac, A.D., Norris, J.R., Lawler, R.G., 1979. Nanosecond time-resolved EPR in-pulse radiolysis via the spin echo method. J. Chem. Phys. 71 (11), 4380–4390.

Tsai, T.E., Griscom, D.L., 1988. Dispersion diffusion transport of radiolytic atomic hydrogen in high-purity hydroxy-containing silica (SiO_2:OH) glass. J. Non-Cryst. Solids 106 (1–3), 374–379.

Tsai, T.E., Griscom, D.L., Friebele, E.J., 1989. Medium-range structural order and fractal annealing kinetics of radiolytic atomic hydrogen in high-purity silica. Phys. Rev. B: Condens. Matter 40 (9), 6374–6380.

Wu, C.-G., Bein, T., 1996. Microwave synthesis of molecular sieve MCM-41. J. Chem. Soc. Chem. Commun. 925–926.